Friction dynamics for curved solid surfaces with long-range elasticity

B. N. J. Persson
Institute für Festkorperforschung, Forschugszentrum-Jülich, D-52425 Jülich, Germany

(Received 23 May 2000; accepted 6 July 2000)

In this work I introduce a model that takes into account the effect of *long range elasticity* and apply it to study the boundary lubrication for *curved solid surfaces*. In particular, I investigate the sliding dynamics when the block and the substrate are separated by a molecular thin lubrication film. The role of elasticity and the origin of stick–slip motion is discussed. © *2000 American Institute of Physics.* [S0021-9606(00)70537-X]

I. INTRODUCTION

Sliding friction is one of the oldest problems in physics and has, undoubtedly, a huge practical importance.[1] In recent years, the ability to produce durable low-friction surfaces and lubricant fluids has become an important factor in the miniaturization of moving components in technologically advanced devices.

Recently, a large number of computer simulations[2,3] and analytical studies of simple model systems[4] have been presented, with the aim to gain insight into the atomistic origin of sliding friction. All the computer simulations we are aware of have used flat surfaces, represented by thin (5–20 Å) solid layers, which could not account for long-range elastic effects (see, e.g., Ref. 2). However, all experiments related to boundary lubrication and sliding friction measured the properties of curved surfaces of mesoscopic or macroscopic dimensions, for which the elastic response to external forces is an essential ingredient determining their properties. For example, in the surface forces apparatus,[5] very thin mica sheets are glued onto two cylindrical glass rods. By bringing the cylinders (rotated by 90° relative to each other) in contact, a common interface is formed, whose shape and size is determined by the elastic deformation of the two solids. Curved surfaces are, of course, also involved in almost every real life sliding system, since even nominally flat surfaces have defects and asperities, and the contact between two macroscopic bodies will always occur in a number of discrete areas (typically of micrometer size). For very smooth surfaces, the asperities will mainly deform elastically, i.e., negligible plastic deformation will occur.

In an earlier work we have introduced a model that takes into account the effect of the *long-range elasticity*, and we have applied it to boundary lubrication of *curved solid surfaces*.[6] In particular, we focused on the *squeezing* dynamics of molecular thin lubrication films. [We considered the nature of the $n \rightarrow n-1$ layering transition (where n is the number of layers of lubrication atoms between the solid surfaces), that occurs with increasing applied pressure.] In this work we apply the same model to investigate the *sliding* dynamics when the block and the substrate are separated by a molecular thin lubrication film.

II. MODEL

The model used in the present computer simulations was described in detail in Ref. 6, and here we only give a short summary. We are concerned with the properties of a lubricant film squeezed between the curved surfaces of two elastic solids. In experiments, a system of this type is obtained by gluing two elastic slabs (of thickness W_1 and W_2) to ''rigid'' surface profiles of arbitrary shape. If the radius of curvatures of the rigid surfaces are large compared to W_1 and W_2, the elastic slabs will deform, reproducing with their free surfaces the (nearly arbitrary) shape of the underlying rigid profiles.

To account for the elastic response of the slabs, without dealing with the large number of atoms required to simulate a mesoscopic elastic solid, in our model we treat at the atomistic level only the last few atomic layers of the solids at the interface. The force constants connecting these atoms to the underlying solid, however, are not the bare parameters, determined by the model interatomic potential. Instead, as described in Ref. 6, those force constants are treated as effective parameters that implicitly reintroduce the elastic response of the slabs of arbitrary width W_1 and W_2.

The atoms in the bottom layer of the block (open circles) form a simple square lattice with lattice constant a, and lateral dimension $L_x = N_x a$ and $L_y = N_y a$. In the following, periodic boundary conditions are assumed in the xy plane.

Between the block and substrate we assume a layer (monolayer or more) of lubrication atoms, which interact with each other via Lennard-Jones pair potentials:

$$v(r) = 4\epsilon_0 \left[\left(\frac{r_0}{r} \right)^{12} - \left(\frac{r_0}{r} \right)^{6} \right].$$

The parameters (ϵ_0, r_0) have been chosen to describe Xe. We also assume that the lubrication atoms interact with the atoms of the solid surfaces via Lennard-Jones pair potentials but with different parameters (ϵ_1, r_1).

In our simulations we shall assume that the block is moving, while the bottom surface of the substrate is fixed in space. To the block is connected an external spring (spring constant k_s) and the ''free'' end of the spring moves with the velocity v_s parallel to the substrate (see Fig. 1). The mass of the sliding block is denoted by M. Before sliding, the system is ''prepared'' by starting with well separated solid surfaces

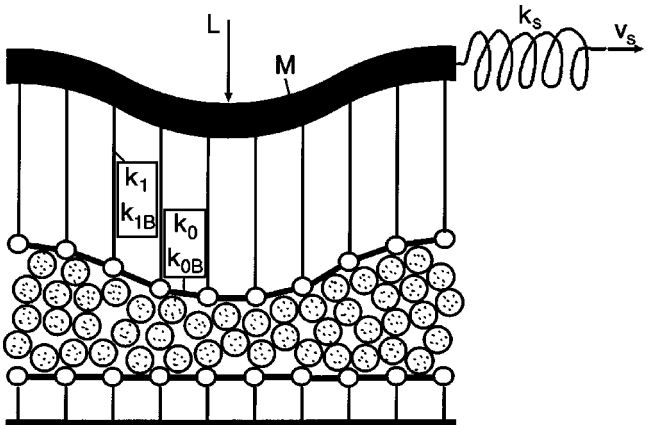

FIG. 1. Schematic picture of the sliding system used in the present paper.

(no atomic contact) covered by the lubrication atoms (corresponding to typically four monolayers of Xe atoms). Next, the upper surface of the block is moved with a (low) constant velocity towards the substrate until the average pressure $P_0 = L/(L_x L_y)$ (where L is the load or normal force) takes some definite predecided value. As described in detail in Ref. 6, this will result in a flattened out region with a well-defined number of Xe-monolayers between the surfaces. In the present case a single Xe-monolayer occurs in the high pressure contact region (see below).

In the simulations presented below, we assumed that the elastic properties of the solids correspond (approximately) to steel. That is, we use $E = 10^{11}$ N/m^2 (elastic modulus), $\nu = 0.3$ (Poisson ratio), and $\rho = 5096$ kg/m^3 (mass density). The block is 100 Å thick and has a cosine corrugation along the x direction, while the substrate is flat and consists of just one monolayer of atoms. The parameters for the interaction among the lubricant atoms ($\epsilon_0 = 20$ meV, $r_0 = 4$ Å and the atomic mass 100) correspond to xenon.

In the computations I have assumed the mass of the block $M = 10^5\, m$ (where m is the Xe-atomic mass) and $r_1 = 1.1\, r_0 = 1.375a$, where a is the common lattice constant of the block and the substrate. We also assume $\epsilon_1 = 3\epsilon_0 = 60$ meV, $N_x = 200$, $N_y = 30$. The number of Xe atoms in the basic unit $N = 14\,000$ correspond to roughly four monolayers of Xe atoms. However, after the surfaces are squeezed together with the (average) pressure $P_0 = 10^9$ Pa, only a single monolayer remains in the flattened out contact area. Thus, most of the Xe-fluid is trapped in the vacancies between the surfaces. All results presented in this paper are for the temperature $T = 200$ K.

Figure 2 shows the potential energy (in eV) (top) and the equilibrium height (in units of the substrate lattice constant a) (bottom) for a Xe atom displaced over the substrate from an on-top site, over the hollow site, to another on-top site (see the inset). The Xe atoms bind strongest in the hollow sites and weakest in the on-top sites. The binding energy in the hollow site is $E_B = 0.46$ eV, and the overall corrugation in the binding potential energy surface equals 13%. The fluctuation in the height of the Xe atom between the hollow and on-top site is $0.08a$. We note, however, that when an adsorbate layer is confined at high pressure between two solid

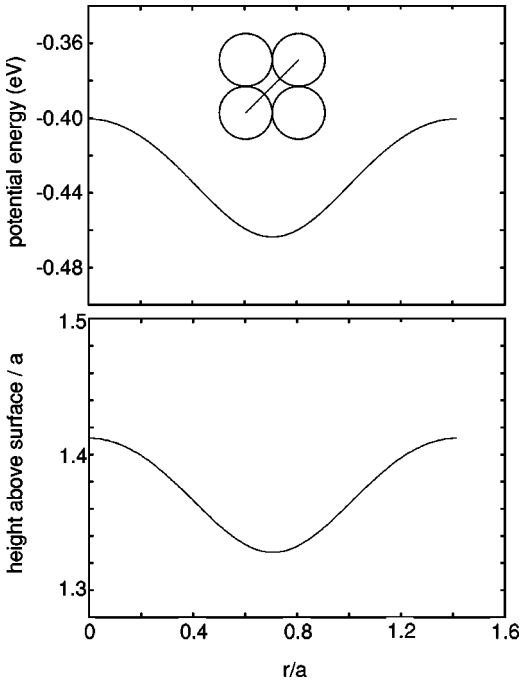

FIG. 2. The potential energy (top) and the height above the surface (bottom) as a function of the lateral position of the Xe atom between on-top–hollow–on-top (see the inset).

surfaces, the effective barrier for diffusion will strongly increase. The substrate lattice constant $a = 3.2$ Å is much smaller than the equilibrium Xe–Xe separation (which is close to $r_0 = 4$ Å). As a result, the Xe-monolayer adsorbed on the substrate forms an incommensurate hexagonal structure.

III. SIMULATION RESULTS

Let us first note the following: The maximum static shear stress observed in the computer simulations presented below is of order $\sigma \sim 10^8$ Pa. Since the shear modulus $G \approx 4 \times 10^{10}$ Pa, it follows that the maximum displacement u ($u \approx \sigma W/G$ in the present case) of the contact area, relative to the center of mass of the block, will be of the order of a few tenths of an Å, i.e., about a factor of 10 smaller than the lattice constant a. Thus, the motion of the bottom surface of the block will closely follow that of the center of mass of the block. However, in most practical cases the displacement u will be much larger than the lattice constant, and in these cases it is possible for the contact area to perform large-amplitude (compared to the lattice constant) stick–slip motion even if the center of mass of the block moves steadily forward with a nearly constant velocity. For example, if the radius of the contact area $R = 10\,\mu$m, then even for an elastically stiff material such as steel, the displacement (see Sec. IV) $u \approx (\sigma/E)R \approx 1000$ Å, i.e., much larger than the lattice constant $a \sim 1$ Å.

Figure 3 shows the kinetic frictional stress as a function of the sliding velocity. Although the spring force is nearly constant, the shear stress acting on the lower surface of the block exhibits periodic oscillations (period T), corresponding to a spatial wavelength $vT = a$, where a is the lattice

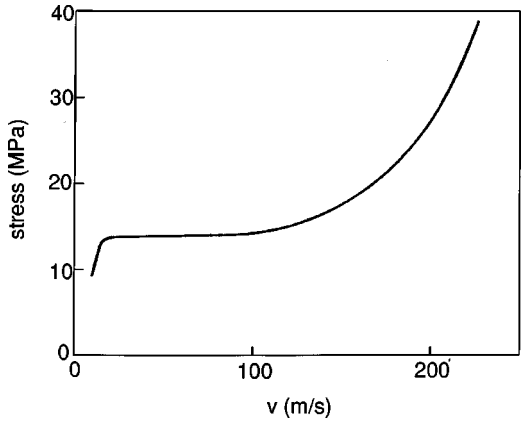

FIG. 3. Kinetic shear stress as a function of the sliding velocity.

constant of the solids. This is illustrated in Fig. 4 which shows (a) the velocity of the bottom surface of the block and (b) the shear stress when the spring velocity $v_s=9$ m/s. (In the simulations the steady state has not yet been reached, and the velocity exhibits some ''long-time'' oscillations.) The stress shown in Fig. 3 has been obtained from simulations of the type illustrated in Fig. 4(b) by averaging over the time period T. Within each period the lubrication film goes from a pinned solid state to an incommensurate sliding state (see Fig. 10), i.e., *the bottom surface of the block performs stick–slip oscillations, even if the center of mass moves (nearly) steadily*. That is, because of the big mass of the block and the high frequency of the stress fluctuations, the effect of the stress fluctuations on the velocity of the block is very small. In macroscopic systems the effect on the center of mass motion will be even smaller, in particular in the multicontact case, where the phase of the stress fluctuations in the different junctions will be nearly uncorrelated. It is interesting to note that, for $v>60$ m/s, the (average) velocity of the lubrication film in the *contact* area equals $v/2$, where v is the center of mass velocity of the block. Thus, the adsorbate layer (in the contact area) slides with the velocity $v/2$ relative to *both* the substrate and the block. However, when v decreases below 60 m/s the (average) velocity of the lubrication film gradually increases towards v, and for $v<30$ m/s, the velocity of the lubrication film equals the velocity of the block. If the block and substrate were identical, this would be a manifestation of a (dynamically) broken symmetry, but in the present case it simply reflects the fact that the block is 100 Å thick, while the substrate consists of just one layer of atoms. This allows the block to deform more easily than the substrate, resulting in a stronger pinning of the lubrication atoms to the bottom surface of the block. In spite of this change in the sliding dynamics in the velocity interval 20 m/s$<v<$60 m/s, there is a negligible variation in the magnitude of the frictional shear stress (see Fig. 3). For $v<20$ m/s, the shear stress drops, but I have not been able to understand the origin of this effect. When the spring velocity is reduced below 9 m/s, the steady sliding motion becomes unstable, and the block performs stick–slip motion. This critical velocity depends in general on the spring constant k_s, and on the mass M of the block. When the velocity v of the block increases, the amplitude of the stick–slip oscillations in the shear stress decreases. At high enough velocity, because of the inertia of the lubrication atoms, the adsorbate layer will not be able to fluctuate between the hexagonal structure and the commensurate domain wall structure, in which case the hexagonal structure should prevail for all time. This type of behavior has been observed in other computer simulations. However, I have not been able to study this limit in the present case since, at very high velocities ($v>240$ m/s), the lubrication film is (rapidly) squeezed out from the contact area.

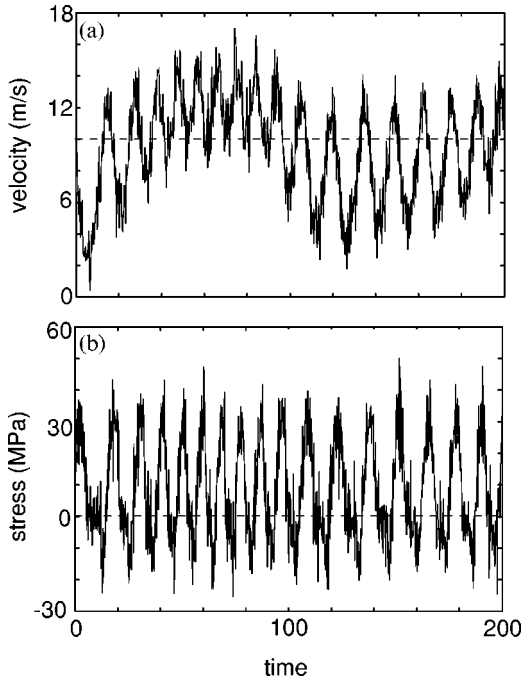

FIG. 4. The (average) velocity of the bottom surface of the block (a) and the shear stress acting on the lower surface of the block from the lubrication atoms (b), as a function of time. The simulations are for a case where (smooth) kinetic sliding is stable and the system approaches constant stress and sliding velocity for increasing time. For $v_s=9$ m/s and $k_s=3$ N/m.

Figure 5 illustrates the influence of acceleration (and retardation) on the shear stress. In this case the spring velocity is so high ($v_s\approx 67$ m/s) that the steady sliding state is stable, but the system has not reached the steady state (the block performs damped oscillations, where the center of mass velocity of the block converges towards $v_s\approx 67$ m/s with increasing time). Time is measured in natural units $[(mr_0^2/\epsilon_0)^{1/2}]$ and the stress and the center of mass velocity of the block have been averaged over a short-time interval $\Delta t=4$. Note that the *frictional shear stress is maximal when the acceleration of the block is maximal* (vertical dashed line), and *minimal when the retardation of the block is maximal*. This result may at first seem surprising, since for the velocities exhibited by the block (see Fig. 5), 20 m/s$<v<$100 m/s, the steady state frictional shear stress is nearly constant (see Fig. 3). However, the explanation for the observed behavior is simple. During acceleration, the Xe fluid in the cavity region between the two surfaces (see Fig. 1) is dragged by the sliding block and will exhibit the same acceleration as the block. Thus, the lubrication fluid will exert a force of inertia on the block, which gives rise to the maxi-

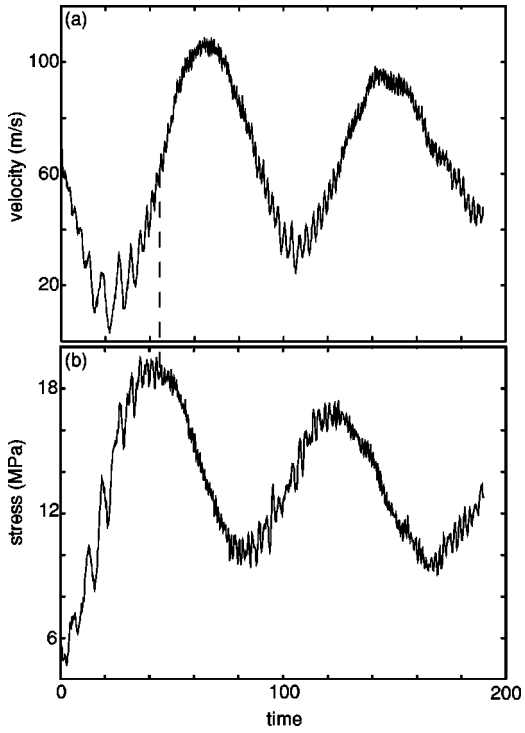

FIG. 5. The sliding velocity of the block (a) and the shear stress acting on the lower surface of the block from the lubrication atoms (b) as a function of time. The simulations are for a case where (smooth) kinetic sliding is stable and the system approaches constant stress and sliding velocity for increasing time. Note that the shear stress is maximum when the acceleration of the block is maximal, while the shear stress is minimal when the retardation of the block is maximal. For $v_s = 66.7$ m/s and $k_s = 3$ N/m.

mum in the friction force during the acceleration of the block. Similarly, during retardation there will be an inertia force on the block from the Xe-fluid, acting in the *opposite* direction to the shear stress in the contact area, and the force on the block from the lubrication layer will therefore take its smallest value when the retardation is maximal.

Figure 6 shows the sliding dynamics when the spring velocity ($v_s = 8.89$ m/s) is so small that the block exhibits stick–slip dynamics. Figure 6(a) shows the spring force as a function of time (in natural units). Note that the spring force becomes negative towards the end of both slip events. This implies that (because of the inertia of the block), the external spring is compressed before the motion of the block stops. Note, however, that there is a fundamental difference between the two slip events displayed in Fig. 6. In the first slip event the motion of the block does not stop when the center of mass velocity vanishes for the first time, which occurs close to the minimum of the spring force, but rather the block continues to slide for a while in the opposite direction. This effect is more clearly displayed in Fig. 6(b) which shows the position of the block as a function of time. Note that the distance the block has slid decreases close to the end of the first slip event. On the other hand, at the second slip event the motion of the block stops when the center of mass velocity vanishes for the first time. I have performed many simulations of stick–slip dynamics and found that these two types of slip events occur with roughly equal probability. The fact that the block does not stop sliding when the center

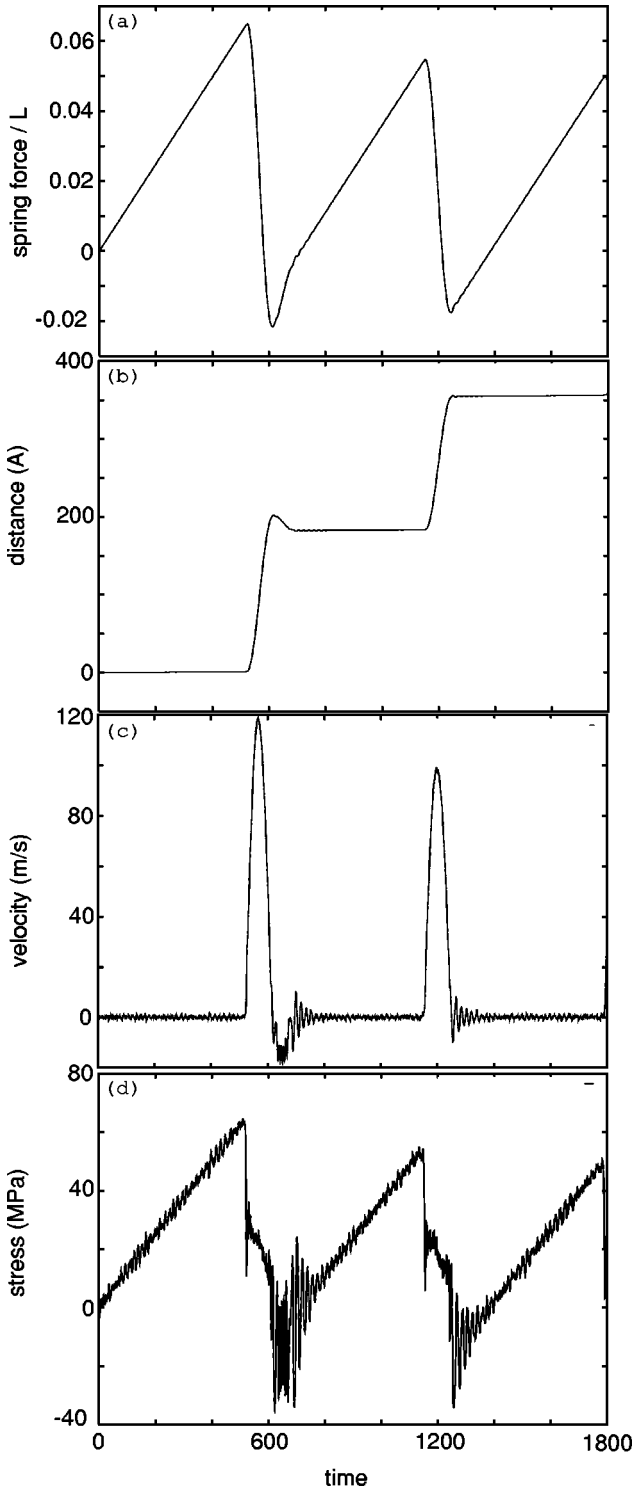

FIG. 6. Stick–slip dynamics. The figure shows (a) the spring force divided by the load L acting on the sliding block, (b) the sliding distance (in Å), (c) the center of mass velocity (in m/s), and (d) the frictional shear stress acting on the lower surface of the block from the lubrication atoms. In the calculations $v_s = 8.89$ m/s and $k_s = 3$ N/m. Time averaged over $\Delta t = 4$.

of mass velocity vanishes for the first time is in drastic contrast to the often assumed classical friction law, where the friction force $F_0 = \pm F_k$ for $v \neq 0$ and $-F_s < F_0 < F_s$ for $v = 0$. Clearly, there is some characteristic relaxation time τ such that if the block spends too short a time (comparing to τ) in the region $v \approx 0$, the lubrication film has no time to

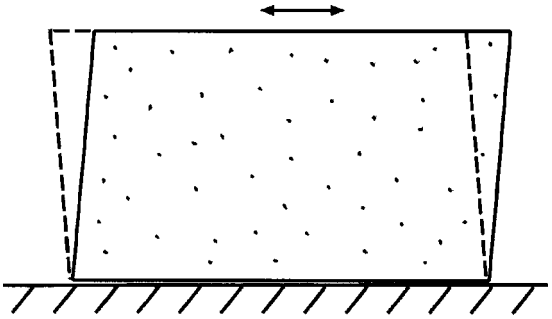

FIG. 7. Mechanical vibration of an elastic block with the bottom surface pinned to the substrate.

relax into the pinned configuration. Figure 6(c) shows the velocity of the center of mass of the block. Note that, in accordance with the discussion above, the velocity is negative close to the end of the first slip event. The damped oscillations in the center of mass velocity (and the shear stress) immediately after the bottom surface of the block

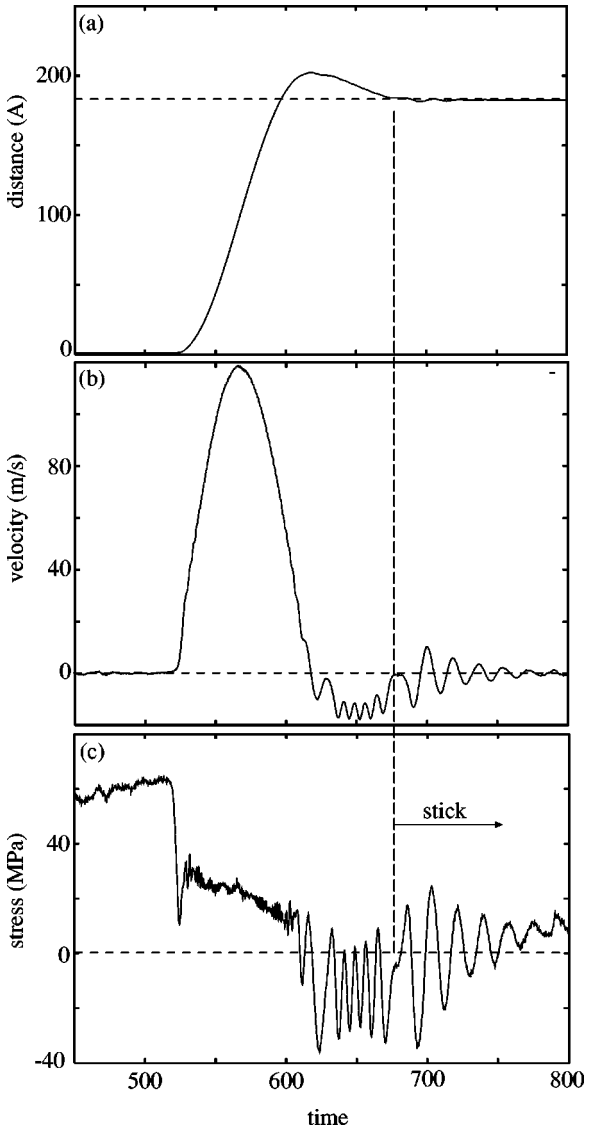

FIG. 8. From Fig. 6 illustrating the transition from stick→slip→stick on an expanded time-scale. Time averaged over $\Delta t=4$.

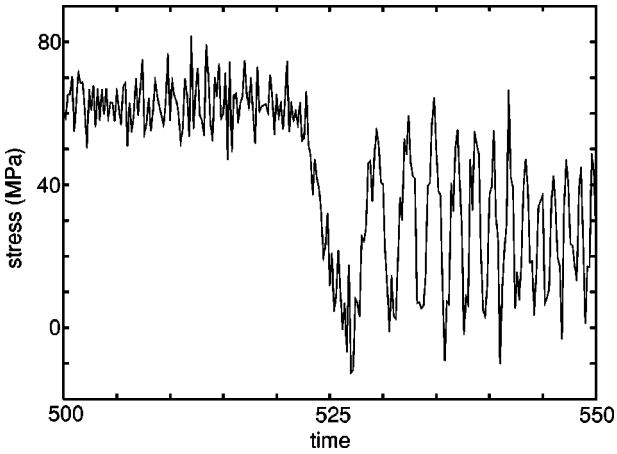

FIG. 9. Illustration of the transition from stick→slip in Fig. 6, on an expanded time scale and without time averaging.

sticks (at the end of both slip events) are due to mechanical vibrations of the block (see Fig. 7) and have recently been observed in surface forces apparatus measurements.[7] Figure 6(d) shows the shear stress acting on the lower surface of the block from the lubrication layer. In this figure, we have again averaged the stress over the time interval $\Delta t=4$.

Figure 8 shows the stick–slip dynamics on an expanded time scale in the vicinity of the onset of the first slip event. We focus first on Fig. 8(c) which shows the shear stress (averaged over $\Delta t=4$). Although the slip velocities are such that one would (from Fig. 3) expect the shear stress to be nearly constant during slip, it decreases monotonically with increasing time. This result is simple to explain: according to Fig. 8(b) the block first accelerates and then retards. The acceleration is maximal very close to the start of slip, after which the acceleration decreases continuously with increasing time. This is followed by a time interval where the block retards, and the retardation is maximal close to the time point where the block reverses ($v<0$) its motion. We have shown above (see Fig. 5) that, because of the inertia of the trapped fluid, during nonsteady slip the frictional stress is maximal when the acceleration is maximal and minimal when the retardation is maximal. This explains the monotonic decrease in the kinetic frictional stress during slip in Fig. 8(c). The oscillations in the shear stress for $t>675$, which start when the bottom surface of the block sticks (at $t=675$) is due to mechanical vibrations of the block (see Fig. 7). Note also the large fluctuations in the shear stress during reverse ($v<0$) slip. This reflects the stick–slip motion of the bottom surface of the block which, as mentioned above, occurs even during steady sliding. Such oscillations also occur during the forward slip ($v>0$) time period, but in this case the sliding velocity, and hence the frequency (in time) of the stress oscillations, is so high that the fluctuations nearly disappeared after the time averaging.

Figure 9 shows the onset of slip on an even more expanded time scale and without time averaging. Note the strong oscillations in the shear stress during slip, and the decrease in the time period T of the oscillations as the speed of the block increases. In each oscillation the bottom surface

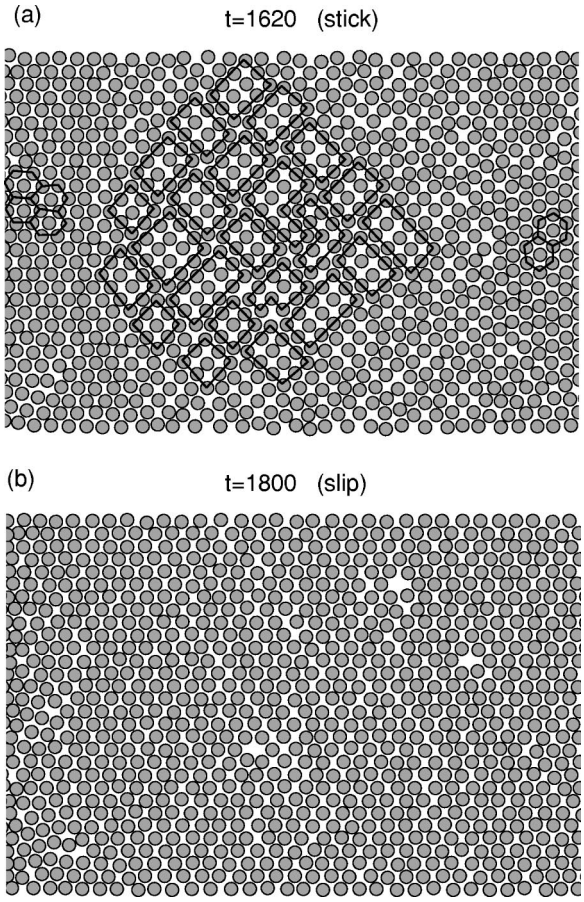

FIG. 10. Snapshot pictures of the central region of the lubrication film (a) at stick and (b) during slip.

of the block displaces a single lattice spacing a so that $vT=a$.

Figure 10 shows snapshot pictures of the adsorbate layer during (a) stick and (b) slip. Note that during slip the lubrication film forms a nearly perfect incommensurate (hexagonal) structure. During stick, the lubrication film in the central (high-pressure) region of the system exhibits a pinned domain wall structure, where small rectangular areas of commensurate $c(2\times 2)$ structure are separated by high-density domain walls. In the periphery of the contact area (but still in the area where a single Xe-layer occurs), the adsorbates form a hexagonal structure. The origin of this effect is as follows: By forming the more open $c(2\times 2)$ structure rather than the high density hexagonal structure, it is possible for the surfaces of the elastic solid to relax slightly towards each other. If the surfaces approach each other by the distance Δz (see Fig. 11) then this will give rise to a gain of elastic energy (per unit area) by $P\Delta z$, where $P(x,y)$ is the local pressure in the contact area. At the periphery of the contact area, P, and thus also the elastic relaxation energy, will vanish, and the lubrication film therefore takes the hexagonal structure (which maximizes the Xe–Xe binding energy) close to the boundary of the contact zone. I note that a similar effect has been observed[6] during the squeeze-out of the lubrication film (say from $n=2$ to $n=1$ Xe monolayers), where a transient structure, which opens the way for the layering transition, is first formed. This structure has a lower density than the initial (hexagonal structure) phase and allows the system to release elastic energy, which is the driving force for the phase transformation. It is also interesting to note that at the end of squeezing (before sliding), a hexagonal layer is formed everywhere, and only after sliding a finite (short) distance, the domain-wall structure is formed in the high pressure region (compare Figs. 21 and 23 in Ref. 6). Thus only after some ''massage'' time period (or sliding distance) does the adsorbate layer reach its final steady-state structure, where the adsorbate concentration in the high-pressure region is lower than that of the original hexagonal structure; similar effects has been observed in surface forces apparatus measurements.[8]

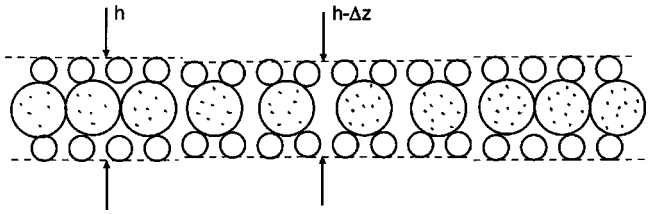

FIG. 11. Schematic picture of the lubrication film at stick. In the central high pressure part of the contact area, the adsorbate layer forms a commensurate structure which allows the solid surfaces to come closer by Δz, resulting in elastic relaxation which is the driving force for the phase transformation. Close to the periphery of the contact area the pressure is low and the adsorbate takes a high-density hexagonal structure which maximizes the Xe–Xe binding energy.

A detailed study of snapshot pictures of the adsorbate layer during the transition from stick to slip shows that slip starts at the periphery of the contact area and propagates rapidly (with a speed of order the sound velocity) towards the center of the contact area. This is the picture one would expect based on continuum elasticity theory. Consider, for example, an elastic sphere squeezed against a rigid substrate. This gives rise to a pressure distribution of the form[9]

$$P\sim[1-(r/R)^2]^{1/2},$$

where R is the radius of the contact area. If, in addition, a tangential force is applied to the elastic sphere, while no slip occurs at the interface, then the tangential stress σ_{xz} will act at the interface, where (approximately)[9]

$$\sigma_{xz}\sim[1-(r/R)^2]^{-1/2}. \tag{1}$$

Thus, in the continuum approximation, an arbitrary weak external tangential force gives rise to an infinite shear stress at the periphery of the contact area. Of course, in an atomistic model the stress remains finite, but it is expected to be largest for $r\approx R$ and the slip should start at the periphery. For $r\approx R$, (1) reduces to $\sigma_{xz}\sim(R-r)^{-1/2}$, which is the same inverse-square-root singularity as exhibited by the stress field in the vicinity of a crack tip, and, in fact, the onset of slip in the present case can be considered as a crack propagating from the periphery of the contact area towards the center.[9]

IV. DISCUSSION

The perhaps most important problem in boundary lubrication is to understand the nature and origin of the transition from slip to stick. Since sliding friction involves buried in-

terfaces, practically nothing is known from direct experimental observation about the the processes which occur in the lubrication layer. In several earlier publications,[1,10,11] we have studied the slip–stick transition theoretically, and in this section we will apply the theory to the computer simulation presented in Sec. III.

The following discussion is based on experimental[8,12] and theoretical[3,13] arguments which suggest that the transition from slip to stick involves nucleation of solid structures in the boundary lubrication film. In the model studied above an incommensurate hexagonal structure prevails during slip while a solid domain wall structure is formed at stick. In some earlier simulations, either an incommensurate structure or a fluidlike structure prevailed during slip.[3] In the latter case the transition from slip to stick involved the nucleation of the solid structure. This scenario is likely to prevail when the lateral corrugation of the adsorbate–substrate interaction potential is ''large,'' and should also be more favorable for ''complex'' lubrication molecules, e.g., long change hydrocarbons (calculations to check this are under way) and for (real) surfaces with defects, e.g., steps, which would tend to break up any solidlike structures in the (sliding) lubrication film. At very low sliding velocity the whole lubrication film is likely to consist of solid domains which fluidize and refreeze in a stochastic manner (see Ref. 13). In this latter case there will be a highly nonuniform stress distribution at the interface, i.e., associated with each solid domain in the lubrication film will be a stress domain in the block and the substrate.[13] However, in all these cases there will be some characteristic relaxation time τ (or a distribution of relaxation times) associated with the strengthening of the junction at stick: in the first two cases, this is associated with the nucleation and growth of the solid pinned structures, while in the latter case, τ characterizes the speed with which the inhomogeneous stress distribution at the interface relaxes towards the stress free state.[13]

In the following discussion we will assume that the spring constant k_s is very weak, in which case the transition from steady sliding to stick–slip motion will occur at a critical sliding velocity v_c, which is independent of k_s and which equals the lowest (steady-state) sliding velocity v_c of the block on a tilted substrate (see Refs. 10 and 11).

Consider a block sliding on a lubricated substrate. Let us consider the formation of a solid domain (island) which pins the two solid walls together. We have shown elsewhere that even if the solid island would be formed instantaneously, there should be no problems related to the inertia of the sliding block. That is, because of the finite elasticity of the solids, it is possible for small surface regions at the interface between the block and the substrate to be pinned abruptly without generating huge shear stresses as a result of the sliding motion of the block. Thus, the initial increase in the shear stress at a solid island (radius r) is associated with the elastic stopping waves generated in the confining solid walls, but the resulting increase in the shear stress is entirely negligible. For times $t > r/c \sim 10^{-11}$ s [where c is the sound velocity, and t the time after the (abrupt) formation of a solid structure with radius r], the shear stress increases monotonically with time. If the increase in the shear force with increasing time is faster than the increase in the pinning force which results from the growth of the solid island, then the solid island will shear melt, and no transition to the stick state can occur.

At the transition from steady sliding to stick, the kinetic energy of the sliding block $Mv^2/2$ must be converted into elastic energy in the lubrication film and in the walls of the block and the substrate. For the system studied in Sec. III, one finds that about half of the energy is stored in the walls and half in the lubrication film. The critical velocity v_c, calculated under the assumption that the block will stop moving when the kinetic energy of the block has decreased to the point that it can be stored as elastic energy in the system without generating so high shear stress at the interface that the solid lubrication layer fluidizes,[10,11] is of order $v_c = 17$ m/s, which is relatively close to the observed critical velocity ≈ 9 m/s. Thus, the present mechanism is likely to be the origin of the transition from slip to stick for the model studied in Sec. III. We have not performed any systematic study of the dependence of the critical velocity on the mass of the block for the model studied in Sec. III, except to notice that v_c increases when the mass M is reduced, in accordance with theory.[10,11]

For more realistic situations, where the radius of the contact area is much larger than in the model study presented in Sec. III, the elastic energy stored in the solid walls will be much more important than the elastic energy stored in the lubrication film at stop. To see this, let us note that the elastic energy stored in the lubrication film is proportional to the contact area $\sim R^2$, while the elastic energy stored in the walls is proportional to the volume $\sim R^3$ (since the elastic deformation field extends a typical distance R into the solids). Thus the ratio of the volume and surface contributions will scale $\sim R$. In a typical application involving the surface forces apparatus, $R \approx 10$–100 μm, which is about 1000 times larger than in the model study presented in Sec. III. Thus, in most cases of practical importance, *the elastic energy stored in the walls will be a factor of 1000 times greater that the elastic energy stored in the lubrication film* (this fact was overlooked in the work by Robbins and Thompson[14]). When this fact is taken into account, the critical velocity v_c calculated under the assumption that the block will stop moving when the kinetic energy of the block has decreased to the point that it can be stored up as elastic energy in the block, is about 1000 times larger than observed by Yoshizawa *et al.*[8] for hexadecane between mica surfaces.[10,11] Thus, the mechanism considered above cannot be the origin of the transition from slip to stick for most real sliding systems.

Let us now present another mechanism for the transition from slip to stick which may be more relevant to practical applications. First, as pointed out above, the transition from slip to stick is likely to involve nucleation of solid structures in the lubrication film. Let us assume that at time $t=0$ a small circular solid region of radius r and area $\Delta A = \pi r^2$ has been formed due to a fluctuation. The solid island pins the two solid walls together. For times $t > 0$ the shear stress increases monotonically with time. As described in Refs. 1, 10 and 11, if this increase in the shear force is faster than the increase in the pinning force which results from the growth

of the solid island, then the solid island will shear melt, and no transition to the stick state will occur.

V. SUMMARY AND CONCLUSION

We have presented results of computer simulations of sliding friction where, for the first time, both long-range elasticity and curved surfaces have been included in a realistic manner. For ''high'' spring velocity v_s steady sliding is observed, while when v_s is lowered below a critical velocity v_c the block performs stick–slip motion. During slip the lubrication film forms a nearly perfect incommensurate (hexagonal) structure. During stick, the lubrication film in the central (high-pressure) region of the system exhibits a pinned domain wall structure, consisting of small rectangular domains of commensurate $c(2\times 2)$ structure, separated by high-density domain walls. By forming the more open $c(2\times 2)$ structure rather than the high-density hexagonal structure, it is possible for the surfaces of the elastic solid to relax slightly towards each other which gives rise to a gain of elastic energy, which is the driving force for the phase transformation. Even during steady motion of the center of mass, the lubrication film fluctuates (with the period determined by the lattice constant a of the solid walls) between a hexagonal structure and the domain wall structure. We have analyzed the sliding dynamics in detail and made several novel observations, e.g., we find that the liquid Xe trapped in the cavities between the solids will result (because of its inertia) in a maximal (kinetic) friction force when the acceleration of the block is maximal, and a minimal friction force when the retardation of the block is maximal.

We are at present extending this work to other lubricants, e.g., chain molecules, as well as solids with different lattice constants and different elastic properties (e.g., soft elastic solids such as rubber). We will also study the influence of different types of surface corrugation on the squeeze-out and sliding dynamics.

ACKNOWLEDGMENT

I acknowledge support by a BMBF grant related to the German–Israeli Project Cooperation ''Novel Tribological Strategies from the Nano-to Meso-Scales.''

[1] B. N. J. Persson, *Sliding Friction: Physical Principles and Applications* (Springer, Heidelberg, 1998); Surf. Sci. Rep. **33**, 83 (1999); J. Krim, Sci. Am. **275**, 74 (1996).
[2] J. Gao, W. D. Luedtke, and U. Landman, Phys. Rev. Lett. **79**, 705 (1997); J. Phys. Chem. B **101**, 4013 (1997); P. A. Thompson and M. O. Robbins, Phys. Rev. A **41**, 6830 (1990).
[3] B. N. J. Persson, Phys. Rev. Lett. **71**, 1212 (1993); Phys. Rev. B **48**, 18140 (1993); J. Chem. Phys. **103**, 3849 (1995).
[4] T. Baumberger, C. Caroli, B. Perrin, and O. Rosnin, Phys. Rev. E **51**, 4005 (1995); B. N. J. Persson, Phys. Rev. B **55**, 8004 (1997); M. Urbakh, L. Daikhin, and J. Klafter, Phys. Rev. E **51**, 2137 (1995); J. M. Carlson and A. A. Batista, Phys. Rev. E **53**, 4153 (1996).
[5] J. N. Israelachvili, *Intermolecular and Surface Forces* (Academic, London, 1995); M. L. Gee, P. M. McGuiggan, and J. N. Israelachvili, J. Chem. Phys. **93**, 1895 (1990); L. Demirel and S. Granick, Phys. Rev. Lett. **77**, 2261 (1996); J. Chem. Phys. **109**, 6889 (1998); J. Klein and E. Kumacheva, Science **269**, 816 (1995); J. Chem. Phys. **108**, 6996 (1998); *ibid.* **108**, 7010 (1998).
[6] B. N. J. Persson and P. Ballone, J. Chem. Phys. **112**, 9524 (2000).
[7] J. Klein (private communication).
[8] H. Yoshizawa, Y.-L. Chen, and J. Israelachvili, Wear **168**, 161 (1993); H. Yoshizawa and J. Israelachvili, J. Phys. Chem. **97**, 11300 (1993).
[9] See, e.g., K. L. Johnson, *Contact Mechanics* (Cambridge University Press, Cambridge, 1985).
[10] B. N. J. Persson and A. I. Volokitin, Surf. Sci. **457**, 345 (2000).
[11] B. N. J. Persson and V. L. Popov, Solid State Commun. **114**, 261 (2000).
[12] A. L. Demirel and S. Granick, in *Physics of Sliding Friction*, edited by B. N. J. Persson and E. Tosatti (Kluwer, Dordrecht, 1996).
[13] B. N. J. Persson, Phys. Rev. B **51**, 13568 (1995).
[14] P. A. Thompson and M. O. Robbins, Science **250**, 792 (1990); **253**, 916 (1991).